Proceedings of the International Conference on Heat Transfer and Fluid Flow
Prague, Czech Republic, August 11-12, 2014
Paper No. 185

Some Investigations on Arachidic Acid/Graphene Composite PCMs

Yoldas Seki, Seyma Ince
Dokuz Eylül University, Department of Chemistry
Tinaztepe, Izmir, Turkey
yoldas.seki@deu.edu.tr; seymaince@gmail.com

Mehmet Uzun, Mehmet Akif Ezan, Levent Cetin, Alpaslan Turgut, Aytunc Erek
Dokuz Eylül University, Department of Mechanical Engineering
Tinaztepe, Izmir, Turkey
mehmed.uz@outlook.com, mehmet.ezan@deu.edu.tr, levent.cetin@deu.edu.tr,
alpaslan.turgut@deu.edu.tr, aytunc.erek@deu.edu.tr

Abstract –This paper aims to examine thermal characteristics of a novel composite PCM that is consist of Arachidic acid and graphene nano-platelets. DSC, TGA and thermal conductivity measurements have been conducted to reveal the influence of graphene loading with various fractions, namely 0.5%, 1.0% and 2.0%. Results reveal that while the graphene loading does not cause any major change on the phase change temperature and the latent heat values even for the long term utilization, significant increment on the thermal conductivity is achieved. It is also evaluated that the degree of sub-cooling decreases with increasing the graphene fraction. Moreover, numerical analyses have been also conducted for three typical capsule geometries, slab, cylinder and sphere, to reveal the influence of the increment of thermal conductivity on the total time for solidification.

***Keywords*:** Arachidic acid, Thermal characterization, Phase change material, Numerical.

1. Introduction

Phase change materials are widely used to provide sustainable usage of thermal energy in both heating and cooling applications. Paraffin, fatty-acids and eutectic mixtures are typical PCMs that are commonly in used. Fatty-acids are known to be appropriate candidate PCMs for latent heat thermal energy storage systems (LHTESS) since possessing the following attractive features; having small or no super-cooling effects during phase change, non-toxic, high heat capacity, congruent melting, lower vapour pressure, non-corrosive to metal container, low cost, good chemical and thermal stability, non-flammability and small volume change (Hasan and Sayigh, 1994; Hasnain, 1998; Sari and Kaygusuz, 2006; Sharma et al., 2009; Yuan et al., 2014). In recent years, researchers are seeking alternative ways to eliminate the major drawback of the fatty-acids, namely possessing lower thermal conductivity. The most common way to improve the thermal conductivity of a PCM is dispersion of highly conductive solid particles, which are in *nano*-size, into the base material. In Fig. 1, a comparative illustration of the results of recent works, that are aimed to adjust the thermal properties of fatty acids, are given. Fauzi et al. (2013) investigated the influence of sodium myristate (SM), sodium palmimate (SP), and sodium stearate (SS) additives into the myristic acid/palmitic acid (MA/PA) eutectic mixture. Results revealed that the addition of 5% SM, 5% SP, and 5% SS into the MA/PA mixture, decreases the degree of sub-cooling and increases the thermal conductivity and the value of latent heat of fusion. Sari et al. (2009) proposed a novel form stable composite PCM which is composed of lauric acid (LA) and expanded perlite (EP). The thermal conductivity of form stable composite PCM has been also enhanced in 84% with the addition of expanded graphite (EG). Wang et al. (2013) aimed to regulate the melting temperature of the capric acid/lauric acid eutectic PCM in order to obtain a novel PCM which is suitable for cold storage. They have indicated that addition of oleic acid with a molar fraction of 0.08 into the eutectic mixture is

adequate to achieve their goal. Yang et al. (2014) prepared a novel PCM which consist of myristic acid/palmitic acid/stearic acid and expanded graphite. It is revealed that addition of expanded graphite increases the thermal conductivity of composite PCM almost 10 times. Zhang et al. (2013) also investigated the influence of expanded graphite on the thermal conductivity of eutectic mixture of lauric acid/myristic acid/palmitic acid.

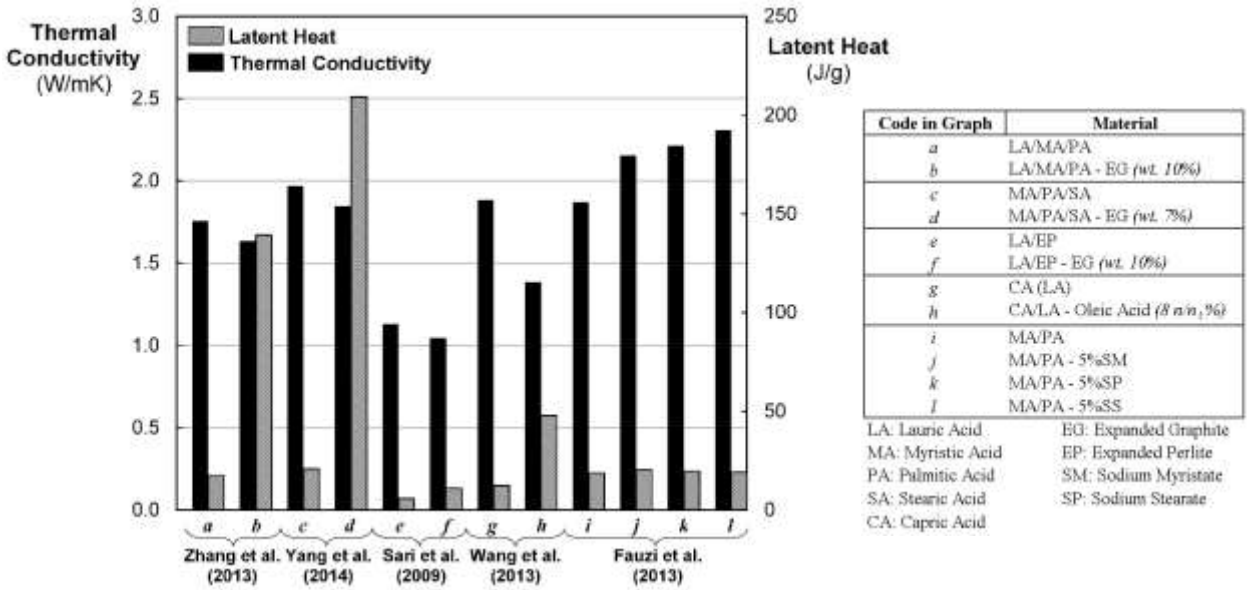

Fig. 1. Recent attempts on improvement the thermal conductivity of fatty acids.

Current study aims to reveal the thermal characteristics and thermal energy storage capacity of a novel PCM, Arachidic acid. Graphene is incorporated into the pure Arachidic acid in various fractions to improve the thermal conductivity value of composite PCM. Numerical analyses are also handled in order to demonstrate the effect of increment on the thermal conductivity of PCM, which is encapsulated in three different types of container; cartesian, cylindrical and spherical.

2. Sample Preparation & Measurements

2. 1. Materials

Arachidic acid (AA) with a purity of 98% was purchased from Alfa Aesar. The chemical formula and molecular weight of AA is $C_{20}H_{40}O_2$ and 312.54 g/mol, respectively. Graphene nano-platelets, with particle size of 5 μm, on the other hand, were supplied from Graphene Chemical Industries, Turkey.

2. 2. Preparation of Arachidic Acid/Graphene Composite PCMs

Graphene nano-platelets in three different mass fractions, 0.5%, 1% and 2%, has been incorporated into the molten AA and the mixture was stirred up with an ultrasonic homogenizer for 3 minutes. Ultimately, the AA/Gr mixture was dried on a petri dish in an oven which is set at 60°C.

2. 3. Thermal Characterization

DSC analyses were carried out with Perkin-Elmer Diamond DSC. Samples were first heated from 65°C to 85°C with a scan rate of 1°C/min. After 1 min isothermal at 85°C, samples were cooled down to the initial temperature with the same scan rate as in heating period and analyses has been finalized after 1 min isothermal at 65°C.

2. 4. Thermal Conductivity Measurements

3ω thermal conductivity measurement technique was used to evaluate the thermal conductivity values of AA and AA/Gr composite PCMs. Method is based on the well-known hot-wire method. A thin metal wire penetrates into a liquid sample may act as a heater and also thermometer. Ni wire with diameter and length of 40 μm and 19.0 mm is used as a thermal probe (ThP). Schematic of the experimental setup is given on Fig. 2, on the other hand, main components of the setup can be seen in Fig. 3. The accuracy of the measurement method has been validated against some well-known pure liquids such as water, ethanol, methanol and ethylene glycol. Comparative results indicated that the accuracy of the current method is within ±2%. Detailed information about the principles of the current measurement system can be found elsewhere (Tavman and Turgut, 2010; Turgut et al., 2008).

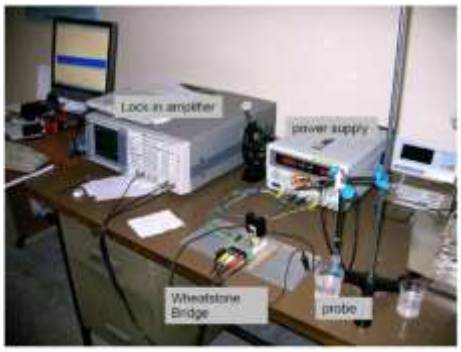

Fig. 2 Schematic diagram of 3ω experimental set-up (Tavman and Turgut, 2010).

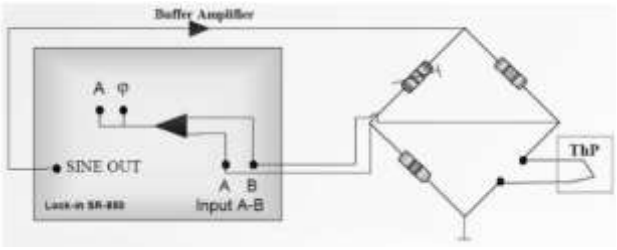

Fig. 3 Main components of the 3ω experimental set-up (Tavman and Turgut, 2010)

3. Numerical Study

3. 1. Definition of the Problem

Three different types of capsule geometries are considered in this study. AA or composite AA/Gr PCMs are assumed to be encapsulated inside a slab, infinite cylinder and a spherical capsule with an identical characteristic length of $2r_o$. Initially, capsules and the PCM are assumed to be at a definite temperature which is higher than the melting temperature of PCM ($T_{in} = T_m + \Delta T$) and then the capsules are suddenly submerged into a constant temperature bath which is maintained at a constant temperature that is below the melting temperature of PCM ($T_\infty = T_m - \Delta T$). Here the temperature range is set as 10 K. It is assumed that the only heat transfer mechanism takes place inside the capsules is one-dimensional heat conduction. Thermo-pyhsical properties of PCMs are assumed to be identical in the solid and liquid phases. For this work, since the evaluation of specific heat and the density of graphene loaded PCMs is out of scope, those properties are assumed to be unchanged with varying the graphene fraction, and defined to be $\rho = 900$ kg/m^3 and $c_p = 2000$ J/kgK. Thanks to the symmetry, computational domain is reduced to be the half of the containers, as illustrated in Fig. 4, and on the symmetry plane, temperature gradient is set to be zero at $r = 0$ ($\partial T/\partial r\big|_{r=0} = 0$). On the other hand, convection takes place at the outer surface of the computational domain, at $r = r_o$, and the related boundary condition can be derived from the energy balance at the interface of the domain as $-k\,\partial T/\partial r\big|_{r=r_o} = h\left(T - T_\infty\right)$. Since the phase change process takes place at a constant temperature, the convective heat transfer coefficient could be defined to be constant as, $h = 400$ W/m^{2}K. It should be also noted that the shell thickness of the container is neglected.

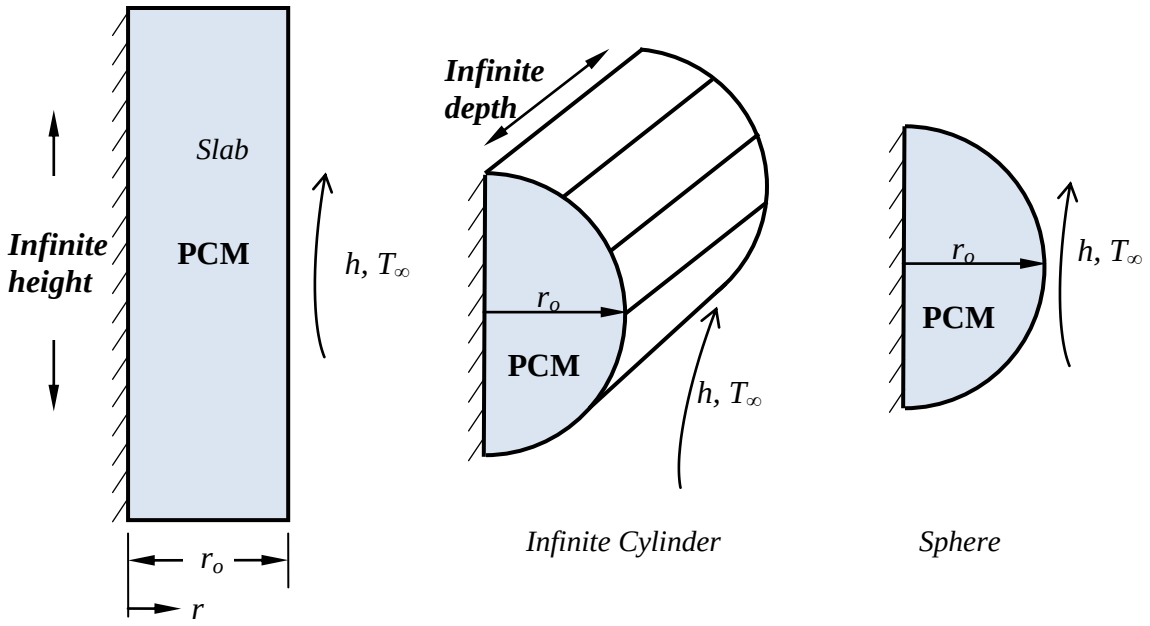

Fig. 4 Computational domains.

3. 2. Governing Equations and Solution Method

One-dimensional enthalpy equation is transformed into temperature based form, as suggested by Cao and Faghri (1990). In order to regulate the sudden variation on the enthalpy during phase change, current method defines the enthalpy as a piece-wise linear functions in terms of temperature as, $H = C^*T + S^*$. Heat capacity ($C^* = \rho c$) and the source term ($S^* = \rho s$) vary depending on the phase of the material (*liquid, mushy or solid*). Mushy zone is defined as a fictitious transition region in which phase change occurs. In the current analyses, temperature range of the mushy zone is selected to be $T_m \pm \delta T_m$ and δT_m is optimised to be 0.01 K. The non-dimensional parameters that are given in Table 1 are used to obtain dimensionless governing equation in Eq. (1).

Table 1. Dimensionless parameters.

$C = (\rho c)/(\rho c)_L$	$K = k/k_L$
$S = (\rho c)/\left[(\rho c)_L (T_{in} - T_m)\right]$	$R = r/r_o$
$\theta = (T - T_m)/(T_{in} - T_m)$	$\tau = \alpha_L t/r_o$
$\mathrm{Ste} = c_L (T_{in} - T_m)/\Delta H$	$\mathrm{Bi} = hr_o/k_L$

$$\frac{\partial}{\partial \tau}(C\theta) + \frac{\partial}{\partial \tau}(S) = \frac{1}{R^n}\frac{\partial}{\partial R}\left(KR^n \frac{\partial \theta}{\partial R}\right) \tag{1}$$

where n = 0, 1, and 2 express geometric form of the equation for cartesian, cylindrical and spherical coordinates, respectively. Besides, C, K and S are defined for each phase of the material as

$$C(\theta)=\begin{cases} C_S & \theta<-\delta\theta_m \\ 0.5(1+C_S)+\dfrac{1}{2\mathrm{Ste}\delta\theta_m} & -\delta\theta_m\le\theta\le+\delta\theta_m \\ 1 & +\delta\theta_m<\theta \end{cases} \tag{2}$$

$$K(\theta)=\begin{cases} K_S & \theta<-\delta\theta_m \\ K_S+(1-K_S)\dfrac{\theta+\delta\theta_m}{2\delta\theta_m} & -\delta\theta_m\le\theta\le+\delta\theta_m \\ 1 & +\delta\theta_m<\theta \end{cases} \tag{3}$$

$$S(\theta)=\begin{cases} C_S\delta\theta_m & \theta<-\delta\theta_m \\ 0.5(1-C_S)\delta\theta_m+0.5/\mathrm{Ste} & -\delta\theta_m\le\theta\le+\delta\theta_m \\ C_S\delta\theta_m+1/\mathrm{Ste} & +\delta\theta_m<\theta \end{cases} \tag{4}$$

Finite volume approach is implemented to discretize the energy equation into sets of algebraic equations. In all cases, total number of computational volumes are set to identical and optimized to be two-hundred. Tri-Diagonal Matrix Algorithm (TDMA) has been used to resolve the matrix. Primarily results are revealed that Δt = 10 s is sufficient enough to capture the time-wise variation of phase change interface. Convergence criteria is defined as the maximum relative difference of temperature values between following iterations and for each time step iterations are carried on until the deviation becomes less than 10^{-14}.

3. 3. Validation the Method

In order to validate the current mathematical model, numerical work of Bilir and Ilken (2005) is reproduced. Bilir and Ilken (2005) considered a spherical container that is filled with water. Initially the sphere is at 25°C, and then suddenly sphere is submerged into a bath which contains ethylene-glycol/water mixture at -25°C. Time-wise variation of the surface temperature is compared in Fig. 5 for the current and reference work.

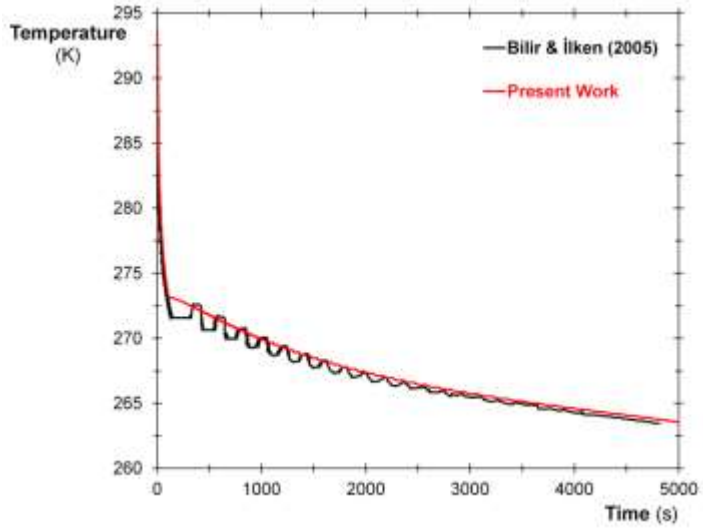

Fig. 5 Comparative work against Bilir and Ilken (2005).

4. Results and Discussion

4. 1. Thermal Characteristics of PCM

Results of the DSC analyses are reported in Table 2 for the pure AA and AA/Gr composite PCMs. While the melting temperature of AA does not change considerably with the graphene treatment, the freezing temperature approaches to the freezing temperature with increasing the graphene fraction, which means that the degree of supercooling decreases with graphene loading. On the other hand, even for the pure AA case, the degree of super-cooling does not change with increasing thermal cycles, for the graphene loaded AA composite PCMs, it is clear that the degree of supercooling drops down almost 0.6°C.

Results also reveal that increasing thermal cycles has almost no effect on the melting or freezing latent heat values. Besides, in comparison to the pure MA, the melting and freezing latent heat values decrease by almost 3% for the composite PCM with 2% graphene loadings.

Table 2. The effect of thermal cycling and graphene loading on the thermal properties of MA.

Sample Code	Number of thermal cycling	Melting temperature (°C)	Melting Latent heat (J/g)	Freezing temperature (°C)	Freezing Latent heat (J/g)	Degree of supercooling $T_m - T_f$ (°C)
Pure AA	1^{st}	76.4	223	74.6	-218	1.8
	40^{th}	75.9	220	73.6	-218	2.3
	100^{th}	75.8	223	73.7	-218	2.1
AA/0.5Gr	1^{st}	77.3	224	75.1	-220	2.2
	40^{th}	76.0	222	75.3	-218	0.7
	100^{th}	76.0	224	75.3	-219	0.7
AA/1.0Gr	1^{st}	76.2	223	75.2	-218	1.0
	40^{th}	75.9	224	75.3	-217	0.6
	100^{th}	75.9	223	75.3	-218	0.6
AA/2.0Gr	1^{st}	76.3	218	75.3	-212	1.0
	40^{th}	76.1	218	75.4	-213	0.7
	100^{th}	76.0	216	75.4	-211	0.6

4. 2. Thermal Conductivity of PCM

In Table 3, thermal conductivities of pure AA, AA/0.5Gr, AA/1.0Gr and AA/2.0Gr are given. It is clear that increasing the graphene loading inside the composite PCM yields an increment on the thermal conductivity values. Thermal conductivity of pure AA is enhanced by 15%, 30% and 43% for graphene fractions of 0.5%, 1% and 2%, respectively.

Table 3. Thermal conductivities of PCMs.

Sample	Thermal conductivity (W/mK)	Standard Deviation
AA	0.178	± 0.01
AA/0.5Gr	0.205	± 0.01
AA/1.0Gr	0.231	± 0.01
AA/2.0Gr	0.255	± 0.01

4. 3. Influence of Graphene Loading and Geometry on Phase Change Period

In Fig. 6, influences of the graphene loading and the container geometry on the time-wise variations of centre temperature of containers are illustrated. It is clear that, time for complete solidification significantly drops with graphene loadings and using spherical container instead of a slab or a cylindrical capsule.

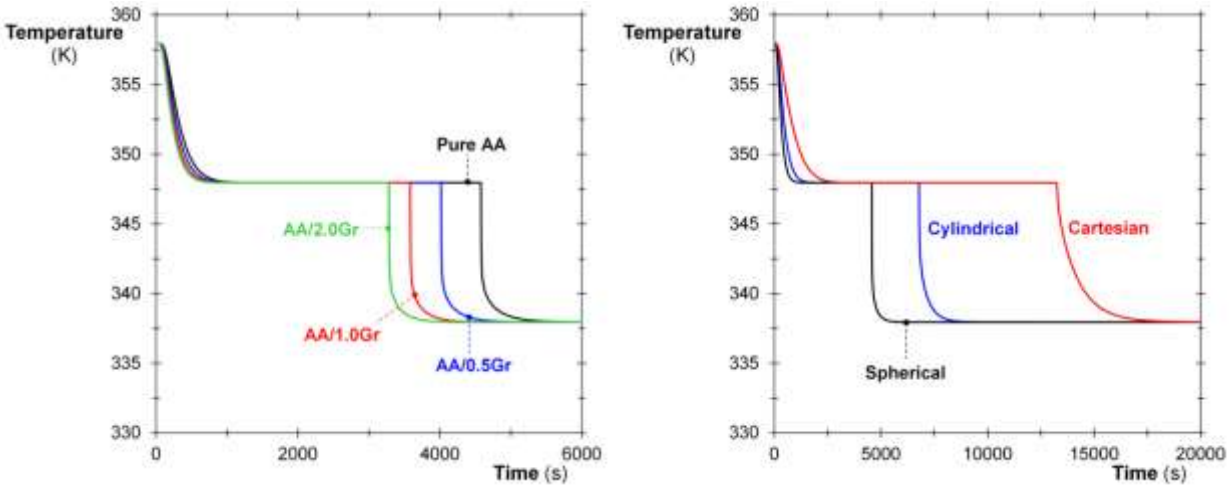

(a) *(b)*

Fig. 6 Influence of (a) Graphene Loading and (b) Container Geometry (*for pure* AA) – *centre temperature*

In Table 4, times for complete solidification are given for each case. One can see that, in comparison to the pure AA case, graphene loading reduces the complete solidification time with fractions of 14%, 27.8% and 39.6% for graphene loading of 0.5%, 1.0% and 2.0%, respectively. On the other hand, geometry of the container also significantly affects the phase change duration. Results reveal that, in comparison to the slab case, cylindrical and spherical containers reduce the time for complete solidification for 95% and 189%, respectively.

Table 4. Influence of Geometry and Graphene Loading on Phase Change Duration.

Geometry	**Time for Complete Solidification (s)**			
	Pure AA	**AA/0.5Gr**	**AA/1.0Gr**	**AA/2.0Gr**
Slab	13259	11628	10373	9498
Cylinder	6786	5951	5309	4862
Sphere	4579	4016	3583	3281

4. Conclusion

As a result of current work, following remarks can be listed;

- Graphene loading tends to increase the thermal conductivity of AA without any significant change in phase change temperature of latent heat of fusion,
- Graphene loading reduces the effect of sub-cooling, in other words, increases the thermal stability of composite PCM.
- 2% of graphene loading inside AA causes a reduction of 40% in complete solidification duration.
- Geometry of containers that are used in latent heat thermal energy storage systems significantly affect the phase change duration.

Acknowledgements

The authors would like to acknowledge the support of the Scientific and Technological Research Council of Turkey (TUBITAK) under Grant No: 112M164.

References

Bilir L., Ilken Z. (2005). Total solidification time of a liquid phase change material enclosed in cylindrical/spherical containers. Applied Thermal Engineering, 25, 1488–1502.

Cao Y., Faghri A. (1990). A Numerical Analysis of Phase Change Problem including Natural Convection, ASME Journal of Heat Transfer. 112, 812-815.

Fauzi H., Metselaar H.S.C., Mahlia T.M.I., Silakhori M., Nur H. (2013). Phase change material: Optimizing the thermal properties and thermal conductivity of myristic acid/palmitic acid eutectic mixture with acid-based surfactants. Applied Thermal Engineering. 60, 261-265.

Hasan A., Sayigh AA. (1994). Some fatty acids as phase-change thermal energy storage materials. Renewable Energy. 4, 69–76.

Hasnain S.M. (1998). Review on sustainable thermal energy storage technologies, Part I: Heat storage materials and techniques. Energy Conversion and Management. 39, 1127–38.

Sari A., Karaipekli A., Alkan C. (2009). Preparation, characterization and thermal properties of lauric acid/expanded perlite as novel form-stable composite phase change material. Chemical Engineering Journal. 155, 899–904.

Sari A., Kaygusuz K. (2006). Thermal Energy Storage Characteristics of Myristic and Stearic Acids Eutectic Mixture for Low Temperature Heating Applications. Chinese Journal of Chemical Engineering. 14, 270–275.

Sharma A, Tyagi VV, Chen CR, Buddhi D. (2009). Review on thermal energy storage with phase change materials and applications. Renewable and Sustainable Energy Reviews. 13, 318-345.

Tavman I., Turgut A. (2010). An investigation on thermal conductivity and viscosity of water based nanofluids. Microfluidics Based Microsystems. 2010, 139–162.

Turgut A., Sauter C., Chirtoc M., Henry J., Tavman S., Tavman I., Pelzl J. (2008). AC hot wire measurement of thermophysical properties of nanofluids with 3ω method. The European Physical Journal-Special Topics. 153, 349–352.

Wang X.L., Zhai X.Q., Wang T., Wang H.X., Yin Y.L. (2013). Performance of the capric and lauric acid mixture with additives as cold storage materials for high temperature cooling application. Applied Thermal Engineering. 58, 252–60.

Yang X., Yuan Y., Zhang N., Cao X., Liu C. (2014). Preparation and properties of myristic–palmitic–stearic acid/expanded graphite composites as phase change materials for energy storage. Solar Energy. 99, 259–66.

Yuan Y, Zhang N, Tao W, Cao X, He Y. (2014). Fatty acids as phase change materials: A review. Renewable and Sustainable Energy Reviews. 29, 482–498.

Zhang N., Yuan Y., Wang X., Cao X., Yang X., Hu S. (2013). Preparation and characterization of lauric–myristic–palmitic acid ternary eutectic mixtures/expanded graphite composite phase change material for thermal energy storage. Chemical Engineering Journal. 231, 214–219.